Adaptive Robust Control of Tele-operated Master-Slave Manipulators with Communication Delay

Nabanita Adhikary, Rajeeb Dey, Muhammad Usman Asad, Jason Gu, Umar Farooq, and Rupak Dutta

Abstract In this paper, a robust controller for the bilateral teleoperation of a master-slave manipulator system is proposed. The controller is designed based on the sliding mode control method with an adaptively tuned gain to tackle the unknown uncertainty bounds of the system. A sliding surface, having a proportional integral derivative type structure, is proposed which is designed as a function of the tracking error between the master and the slave trajectory. The controller design constraints and parameter selection criteria are derived based on the analysis of the closed-loop system. The proposed method is validated using simulation performed for a master-slave system with each arm having two degrees of freedom (DoF) and a constant communication delay for position tracking of the system. The simulation shows that the controller can handle delay of up to 2.5 s while giving satisfactory tracking performance.

Supported by SPARC, MHRD.

N. Adhikary (✉) · R. Dey
Department of Electrical Engineering, National Institute of Technology Silchar, Silchar, India
e-mail: nabanita@ee.nits.ac.in

R. Dey
e-mail: rajeeb@ee.nits.ac.in

M. U. Asad · J. Gu · U. Farooq
Electrical & Computer Engineering, Dalhousie University, Halifax, Canada
e-mail: mh549096@dal.ca

J. Gu
e-mail: Jason.gu@dal.ca

U. Farooq
e-mail: umar.farooq@dal.ca

R. Dutta
Mathematics Department, NIT Agartala, Agartala, India

J. Gu et al. (eds.), *Communication and Control for Robotic Systems*, Smart Innovation, Systems and Technologies 229, https://doi.org/10.1007/978-981-16-1777-5_8

1 Introduction

In recent times due to the advancement of network communication and robotic systems, teleoperated robot manipulator systems have gained worldwide popularity in various applications such as remote surgery, robotic rehabilitation, disaster management, etc. In most of these applications, the manipulators are set up as master and slave devices whose motion and interaction forces require synchronization. To establish this synchronous motion, controllers are required in both the master and the slave devices. Such controller design is a challenging task since the robot manipulators are nonlinear systems, and in addition to this, the communication channel delay adds to the complexity of the problem.

Some recent works in the control of such bilateral system involves application of robust control [3], fuzzy logic [10], neural networks [13], adaptive control [12], etc. Among these methods, robust controllers, especially sliding mode controllers [4, 5], are widely used for such systems owing to their inherent robustness and capability to provide finite-time convergence.

In [7], an adaptive finite-time controller is proposed where a non-singular fast terminal sliding mode controller is used for the bilateral manipulation. The maximum delay bounds used in the paper is 0.7 s. In [9], a state observer-based sliding mode controller with finite-time convergence properties are used in presence of a time-varying delay with a maximum bound of 0.5 s, and their experimental results show the efficacy of the controller within this delay bound. In [14], Zhao et al. proposed an observer-based sliding mode controller with an integral sliding surface that can tackle delays up to 200 ms in an experimental setup and presence of uncertainties. In [8], Wang et al. have proposed an anti-jittering scheme with finite-time controller for a master-slave system with jittering delay. The literature shows that the application of sliding mode control can significantly improve system performance. However, tackling a larger delay is still an open problem, as the controller performance deteriorates with increasing delay.

In this paper, an adaptive sliding mode control law is proposed for a teleoperated dual manipulator system in presence of communication delay. It is assumed that both position and velocity information are available. The controller gain is tuned adaptively where the gain dynamics are proportional to the sliding variable. This allows the user to operate the system in presence of an unknown bound of uncertainty. Moreover, the gain adaptation eliminates the chattering in the control input. The rest of the paper is structured as follows: in Sect. 2, the manipulator model is introduced, and the objective of the controller is defined. In Sect. 3, the controller design and analysis are described. The simulation results are presented in Sect. 4, and the conclusion is given in Sect. 5.

2 Problem Formulation

2.1 System Dynamics

The dynamics of the n-DoF master-slave manipulator system are given as follows:

$$\boldsymbol{M_m}(\boldsymbol{q_m})\ddot{\boldsymbol{q}}_{\boldsymbol{m}} + \boldsymbol{C_m}(\boldsymbol{q_m}, \dot{\boldsymbol{q}}_{\boldsymbol{m}})\dot{\boldsymbol{q}}_{\boldsymbol{m}} + \boldsymbol{G_m}(\boldsymbol{q_m}) = \boldsymbol{u_m} + \boldsymbol{\tau_h} + \boldsymbol{d_m}(\boldsymbol{q_m}, \dot{\boldsymbol{q}}_{\boldsymbol{m}}) \tag{1a}$$

$$\boldsymbol{M_s}(\boldsymbol{q_s})\ddot{\boldsymbol{q}}_{\boldsymbol{s}} + \boldsymbol{C_s}(\boldsymbol{q_s}, \dot{\boldsymbol{q}}_{\boldsymbol{s}})\dot{\boldsymbol{q}}_{\boldsymbol{s}} + \boldsymbol{G_s}(\boldsymbol{q_s}) = \boldsymbol{u_s} - \boldsymbol{\tau_e} + \boldsymbol{d_s}(\boldsymbol{q_s}, \dot{\boldsymbol{q}}_{\boldsymbol{s}}) \tag{1b}$$

where m and s indicates master and the slave robots, respectively, $\boldsymbol{q_i}, \dot{\boldsymbol{q}}_{\boldsymbol{i}}, \ddot{\boldsymbol{q}}_{\boldsymbol{i}} \in \mathbb{R}^{\boldsymbol{n}}$, $i = m(master), s(slave)$ are the angular position, velocity, and acceleration of the manipulator joints, respectively. $\boldsymbol{M_i}(\boldsymbol{q_i}) \in \mathbb{R}^{\boldsymbol{n \times n}}$, $i = m, n$ is the system inertia matrix, $\boldsymbol{C_i}(\boldsymbol{q_i}, \dot{\boldsymbol{q}}_{\boldsymbol{i}} \in \mathbb{R}^{\boldsymbol{n \times n}}$, $i = m, n$ represents the effects Coriolis friction and the centrifugal forces, $\boldsymbol{G_i}(\boldsymbol{q_i}) \in \mathbb{R}^{\boldsymbol{n}}$, $i = m, n$ is the effect of gravitational force, $u_i \in \mathbb{R}^n$, $i = m, n$ is the input torque in the manipulator joints, $\boldsymbol{\tau_h} \in \mathbb{R}^{\boldsymbol{n}}$ is the torque exerted by the operator on the master device and $\boldsymbol{\tau_e} \in \mathbb{R}^n$ is the environmental interaction torque affecting the slave device and $\boldsymbol{d_i}(\boldsymbol{q_i}, \dot{\boldsymbol{q}}_{\boldsymbol{i}}) \in \mathbb{R}^{\boldsymbol{n}}$, $i = m, n$ are the lumped uncertainties affecting the devices. For the current work, it is assumed that there is no environmental or external interaction of the slave manipulator, i.e., $\boldsymbol{\tau_e} = \boldsymbol{0_{n \times 1}}$.

Both the master and slave manipulators are assumed to have the same structure, and the manipulator matrices are as follows [11]:

$$\boldsymbol{M_i}(\boldsymbol{q_i}) = \begin{bmatrix} (m_{1i} + m_{2i})l_{1i}^2 + m_{2i}l_{2i}^2 + 2m_{2i}l_{1i}l_{2i}\cos(q_{2i}) & m_{2i}l_{2i}^2 + m_{2i}l_{1i}l_{2i}\cos(q_{2i}) \\ m_{2i}l_{2i}^2 + m_{2i}l_{1i}l_{2i}\cos(q_{2i}) & m_{2i}l_{2i}^2 \end{bmatrix} \tag{2a}$$

$$\boldsymbol{C_i}(\boldsymbol{q_i}, \dot{\boldsymbol{q}}_{\boldsymbol{i}}) = \begin{bmatrix} -2m_{2i}l_{1i}l_{2i}\dot{q}_{2i}\sin(q_{2i}) & -m_{2i}l_{1i}l_{2i}\dot{q}_{2i}\sin(q_{2i}) \\ m_{2i}l_{1i}l_{2i}\dot{q}_{1i}\sin(q_{2i}) & 0 \end{bmatrix} \tag{2b}$$

$$\boldsymbol{G_i}(\boldsymbol{q_i}) = \begin{bmatrix} (m_{1i} + m_{2i})gl_{1i}\sin(q_{1i}) + m_{2i}gl_{2i}\sin(q_{1i} + q_{2i}) \\ m_{2i}g\sin(q_{1i} + q_{2i}) \end{bmatrix} \tag{2c}$$

The manipulator Jacobian is

$$\boldsymbol{J_i}(\boldsymbol{q_i}) = \begin{bmatrix} -l_{1i}\sin(q_{1i}) - l_{2i}\sin(q_{1i} + q_{2i}) & -l_{2i}\sin(q_{1i} + q_{2i}) \\ l_{1i}\cos(q_{1i}) + l_{2i}\cos(q_{1i} + q_{2i}) & l_{2i}\cos(q_{1i} + q_{2i}) \end{bmatrix} \tag{3}$$

where $i = m(master), s(slave)$.

State Space Representation

The nominal form of the manipulator dynamics described in (1a) and (1b) without considering the unknown uncertainties can be rewritten as

$$\begin{aligned} \ddot{\boldsymbol{q}}_m =& \boldsymbol{M}_m^{-1}(\boldsymbol{q}_m)[-\boldsymbol{C}_m(\boldsymbol{q}_m, \dot{\boldsymbol{q}}_m)\dot{\boldsymbol{q}}_m - \boldsymbol{G}_m(\boldsymbol{q}_m) + \boldsymbol{\tau}_h + \boldsymbol{d}_m(\boldsymbol{q}_m, \dot{\boldsymbol{q}}_m)] \\ &+ \boldsymbol{M}_m^{-1}(\boldsymbol{q}_m)\boldsymbol{u}_m \end{aligned} \tag{4a}$$

$$\ddot{\boldsymbol{q}}_s = \boldsymbol{M}_s^{-1}(\boldsymbol{q}_s)[-\boldsymbol{C}_s(\boldsymbol{q}_s, \dot{\boldsymbol{q}}_s)\dot{\boldsymbol{q}}_s - \boldsymbol{G}_s(\boldsymbol{q}_s) + \boldsymbol{d}_s(\boldsymbol{q}_s, \dot{\boldsymbol{q}}_s)] + \boldsymbol{M}_s^{-1}(\boldsymbol{q}_s)\boldsymbol{u}_s \tag{4b}$$

Considering the state variables for the system as $\boldsymbol{x}_{1i} = \boldsymbol{q}_i \in \mathbb{R}^n$, $\boldsymbol{x}_{2i} = \dot{\boldsymbol{q}}_i \in \mathbb{R}^n$, $i = m, s$ the dynamics for the master and the slave manipulator in the state space form can be written as follows:

$$\begin{aligned} \dot{\boldsymbol{x}}_{1i} =& \boldsymbol{x}_{2i} \\ \dot{\boldsymbol{x}}_{2i} =& \boldsymbol{f}_i(\boldsymbol{x}_{1i}, \boldsymbol{x}_{2i}) + \boldsymbol{g}_i(\boldsymbol{x}_{1i}, \boldsymbol{x}_{2i})\boldsymbol{u}_i \end{aligned} \tag{5}$$

where $i = m, s$, $\boldsymbol{x}_i = [\boldsymbol{x}_{1i}^T \ \boldsymbol{x}_{2i}^T]^T \in \mathbb{R}^{2n}$ are the state variables and

$$\begin{aligned} \boldsymbol{f}_m =& \boldsymbol{M}_m^{-1}(\boldsymbol{q}_m)[-\boldsymbol{C}_m(\boldsymbol{q}_m, \dot{\boldsymbol{q}}_m)\dot{\boldsymbol{q}}_m - \boldsymbol{G}_m(\boldsymbol{q}_m) + \boldsymbol{\tau}_h] \in \mathbb{R}^n \\ \boldsymbol{g}_m =& \boldsymbol{M}_m^{-1}(\boldsymbol{q}_m) \in \mathbb{R}^n \\ \boldsymbol{f}_s =& \boldsymbol{M}_s^{-1}(\boldsymbol{q}_s)[-\boldsymbol{C}_s(\boldsymbol{q}_s, \dot{\boldsymbol{q}}_s)\dot{\boldsymbol{q}}_s - \boldsymbol{G}_s(\boldsymbol{q}_s)] \in \mathbb{R}^n \\ \boldsymbol{g}_s =& \boldsymbol{M}_s^{-1}(\boldsymbol{q}_s) \in \mathbb{R}^n \end{aligned}$$

Some assumptions for the considered master-slave manipulator set are as follows:

Assumption 1 All the joints of both the manipulator are revolute.

Assumption 2 The parametric uncertainty and the external disturbances are bounded, i.e.,

$$|\boldsymbol{d}_m(\boldsymbol{q}_m, \dot{\boldsymbol{q}}_m)| \leq \bar{\boldsymbol{d}}_m \tag{7a}$$

$$|\boldsymbol{d}_s(\boldsymbol{q}_s, \dot{\boldsymbol{q}}_s)| \leq \bar{\boldsymbol{d}}_s \tag{7b}$$

where $\bar{d}_m$ and $\bar{d}_s$ are real valued and absolute value and inequality are taken element-wise.

Assumption 3 The external forces applied to the devices by the user are bounded, which means,

$$|\boldsymbol{\tau}_h(t)| \leq \boldsymbol{\rho}, \ \boldsymbol{\rho} \in \mathbb{R}^n \tag{8}$$

Here, absolute value and inequality are taken element-wise.

Assumption 4 The manipulator joint position, velocity, and accelerations are bounded owing their the mechanical structures and the actuator limits, i.e.,

$$|\boldsymbol{q_i}(t)| \le \bar{\boldsymbol{q}}_i, \quad \bar{\boldsymbol{q}}_i \in \mathbb{R}^n \tag{9a}$$

$$|\dot{\boldsymbol{q}}_i(t)| \le \bar{\dot{\boldsymbol{q}}}_i, \quad \bar{\dot{\boldsymbol{q}}}_i \in \mathbb{R}^n \tag{9b}$$

$$|\ddot{\boldsymbol{q}}_i(t)| \le \bar{\ddot{\boldsymbol{q}}}_i, \quad \bar{\ddot{\boldsymbol{q}}}_i \in \mathbb{R}^n \tag{9c}$$

Here, absolute value and inequality are taken element-wise.

Assumption 5 There are no interaction with the external environment by the slave manipulator.

Some important properties of the robot manipulator are [6]

Proposition 1 *The inertia matrix is bounded, symmetric, and positive definite, and due to assumption (1), the bounds can be expressed as follows:*

$$m_{0i}\boldsymbol{I_n} \le |\boldsymbol{M_i}(\boldsymbol{q_i})| \le m_{1i}\boldsymbol{I_n} \tag{10}$$

$$\bar{m}_{0i}\boldsymbol{I_n} \le |\boldsymbol{M_i^{-1}}(\boldsymbol{q_i})| \le \bar{m}_{1i}\boldsymbol{I_n} \tag{11}$$

$$\mu_{\min}||\boldsymbol{x}||^2 \le \boldsymbol{x^T}\boldsymbol{M_i}(\boldsymbol{q_i})\boldsymbol{x} \le \mu_{\max}||\boldsymbol{x}||^2 \tag{12}$$

where $i = m, n$, $\boldsymbol{x} \in \mathbb{R}^n$ is an arbitrary vector and $0 < \mu_{\min} < \mu_{\max} \in \mathbb{R}$ and $\boldsymbol{I_n}$ is an $n \times n$ identity matrix.

Proposition 2 *The manipulator system is passive which means*

$$\boldsymbol{x^T}\left(\frac{\boldsymbol{1}}{\boldsymbol{2}}\dot{\boldsymbol{M}}_i(\boldsymbol{q}_i) - \boldsymbol{C}_i(\boldsymbol{q}_i, \dot{\boldsymbol{q}}_i)\right)\boldsymbol{x} = 0, \forall \boldsymbol{x} \neq 0, \boldsymbol{x} \in \mathbb{R}^{\boldsymbol{n}}. \tag{13}$$

2.2 Objective

The purpose of this research is to establish a synchronized motion between the master and the slave manipulator when a motion is created in the master manipulator by applying an external force, and the slave manipulator has to follow the trajectory of the master manipulator.

The position tracking errors are defined as

$$\boldsymbol{e_m}(\boldsymbol{t}) = \boldsymbol{q_m}(\boldsymbol{t}) - \boldsymbol{q_s}(\boldsymbol{t} - \boldsymbol{h}) \tag{14a}$$

$$\boldsymbol{e_s}(\boldsymbol{t}) = \boldsymbol{q_s}(\boldsymbol{t}) - \boldsymbol{q_m}(\boldsymbol{t} - \boldsymbol{h}) \tag{14b}$$

The velocity tracking errors are defined as

$$\dot{\boldsymbol{e}}_m(t) = \dot{\boldsymbol{q}}_m(t) - \dot{q}_s(t-h) \tag{14c}$$

$$\dot{\boldsymbol{e}}_s(t) = \dot{\boldsymbol{q}}_s(t) - \dot{q}_m(t-h) \tag{14d}$$

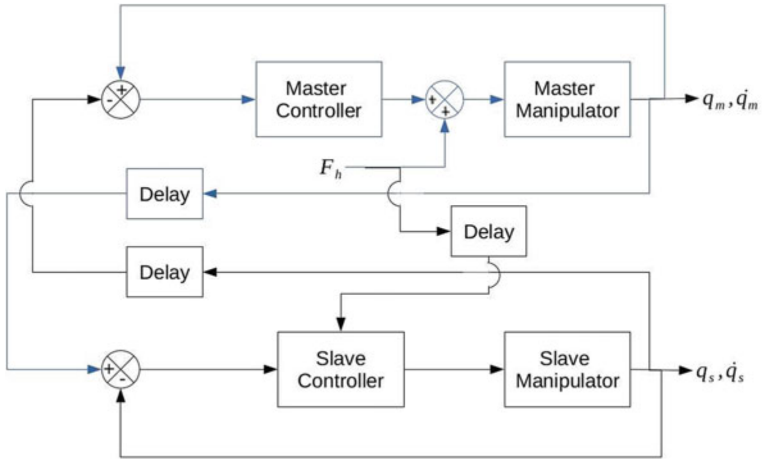

Fig. 1 Block diagram of the tele-operated bi-directional master-slave manipulator

The detailed block diagram of the teleoperated bi-directional master-slave manipulator is shown in Fig. 1. An external force $\boldsymbol{F_h(t)}$ will be applied to the master manipulator such that $\boldsymbol{\tau_h(t) = J_m^T(q_m)F_h(t)}$ that will create a motion in the master manipulator. The movement of the master manipulator is transmitted to the slave manipulator which is expected to follow the motion of the master robot arm. It is assumed that there is no environmental interaction in the slave manipulator side, i.e., $\boldsymbol{\tau_e(t) = 0}$. The transmission channel between the master and the slave side is assumed to have communication delays. Thus, the objective is to design robust feedback controllers for both master and slave manipulators such that the motion created in the master manipulator by the external force is synchronously followed by the slave manipulator in presence of the communication delay, and the resulting system is stable. Thus, the objectives can be summarized as the following points:

1. The motion of the master will be directed by the external force $\boldsymbol{F_h(t)}$ applied by the operator, and this motion will be followed by the slave manipulator. Only the position and velocity information from the master side will be transmitted to the slave side.
2. The tracking errors $\boldsymbol{\dot{e}_m(t)}$ and $\boldsymbol{\dot{e}_s(t)}$ should converge to zero.

3 Controller Design

A sliding mode controller with adaptive gain and a sliding surface having the proportional integral derivative (PID) structure will be designed for the above-mentioned system. Due to the communication delay, at any time instant on both the master and slave sides, the delayed information of the other side is available. Hence on both sides, the tracking error will be considered as the difference between the current information and the delayed information from the other side.

3.1 Sliding Surface Design

The position tracking errors are defined as

$$\boldsymbol{e_m(t)} = \boldsymbol{q_m(t) - q_s(t-h)} \tag{15a}$$

$$\boldsymbol{e_s(t)} = \boldsymbol{q_s(t) - q_m(t-h)} \tag{15b}$$

The velocity tracking errors are defined as

$$\dot{\boldsymbol{e}}_m(t) = \dot{\boldsymbol{q}}_m(t) - \dot{q}_s(t-h) \tag{16a}$$

$$\dot{\boldsymbol{e}}_s(t) = \dot{\boldsymbol{q}}_s(t) - \dot{q}_m(t-h) \tag{16b}$$

On both sides, a variable $\sigma_i(t),\ i = m, s$ is defined as follows

$$\boldsymbol{\sigma_i(t)} = \dot{\boldsymbol{e}}_i\boldsymbol{(t)} + \boldsymbol{C_1 e_i(t)} \tag{17}$$

where $\boldsymbol{C_1} = \text{diag}\{c_{1j}\},\ j = 1, \ldots, n$ is a user-defined positive definite matrix, $i = m, s$.

Thus, the sliding surface for the master manipulator is defined as

$$\boldsymbol{s_m(t)} = \dot{\boldsymbol{e}}_m\boldsymbol{(t)} + \boldsymbol{C_2}\int_0^t \boldsymbol{\sigma_m(\theta)}\mathrm{d}\boldsymbol{\theta}. \tag{18}$$

where $\boldsymbol{C_2} = \text{diag}\{c_{2j}\},\ j = 1, \ldots, n$ is a user-defined positive definite matrix and $\boldsymbol{A}$ is a diagonal matrix with diagonal elements ≤ 1, such that $||\boldsymbol{A}|| \leq 1$.

The sliding surface for the slave manipulator is defined as

$$\boldsymbol{s_s(t)} = \dot{\boldsymbol{e}}_s\boldsymbol{(t)} + \boldsymbol{C_2}\int_0^t \boldsymbol{\sigma_s(\theta)}\mathrm{d}\boldsymbol{\theta}. \tag{19}$$

Analysis of the Sliding Mode Dynamics: The stable dynamics of the sliding surfaces, $\boldsymbol{s_m(t) = 0}$ and $\boldsymbol{s_s(t) = 0}$, will make sure that the tracking error for the master, and slave manipulator motions converges to zero, i.e., objective (2.2) is satisfied. Considering the sliding surface defined for the master manipulator in (18) and using (17), (15a) and (16a), the dynamics of the sliding surface can be defined as follows:

$$\boldsymbol{s_m(t)} = \mathbf{0} \tag{20}$$

$$\dot{\boldsymbol{e}}_m(t) + C_2 e_m(t) + C_1 C_2 \int e_m(t)\mathrm{d}t = 0 \tag{21}$$

Considering $\boldsymbol{z_1 = \int e_m(t)}\mathrm{d}\boldsymbol{t}$, $\boldsymbol{z_2 = e_m(t)}$, the dynamics of (21) can be written as follows:

$$\begin{aligned} \dot{z}_1 &= \boldsymbol{z_2} \\ \dot{z}_2 &= \boldsymbol{-C_2 z_2 - C_1 C_2 z_1} \end{aligned} \tag{22}$$

The dynamics represented by (22) can be rendered stable with the proper selection of controller parameters $\boldsymbol{C_1}$ and $\boldsymbol{C_2}$. Thus, it shows that when $\boldsymbol{s_m(t)} = 0$ is stable, the surface dynamics will cause $\boldsymbol{z_1}$ and $\boldsymbol{z_2}$ to converge to zero, which again using (17) leads to $\boldsymbol{\sigma_i}$ to converge to zero.

3.2 Control Law

Sliding mode control laws for both the master and slave manipulator will be designed as follows:

$$\boldsymbol{u_i} = \boldsymbol{u_{eq(i)} + u_{sw(i)}} \tag{23}$$

where $i = m, s$. Here $\boldsymbol{u_{eq(i)}}$ is the equivalent control which will maintain the sliding dynamics and $\boldsymbol{u_{sw(i)}}$ is the switching control which brings the system dynamics to the sliding surface and compensates for any deviations occurring due to disturbances or change of references.

It is important to note that sensing the angular acceleration is expensive and taking derivative of the velocity signal to obtain the acceleration leads to a highly noisy signal, often unusable. Moreover, using such a noise corrupted and delayed acceleration signal in the control law can cause unnecessary complications in the control input such as the rise of the unaccounted high-frequency dynamics which can prove to be harmful to the system. Hence, while designing the control law, $\ddot{\boldsymbol{q}}_s\boldsymbol{(t-h)}$ is assumed to be unavailable and considered as uniformly zero.

The control law for the master manipulator is as follows:

$$\boldsymbol{u_m(t)} = \boldsymbol{M_m(q_m)}\left[\boldsymbol{-K_m}\mathrm{sign}(\boldsymbol{s_m(t)}) - \boldsymbol{W s_m(t) - C_2 \sigma_m(t)}\right] \tag{24}$$

$$+\boldsymbol{C_m(q_m, \dot{q}_m)\dot{q}_m + G_m(q_m)} \tag{25}$$

where $\boldsymbol{K_m} = \mathrm{diag}\{k_{mi}\}$ and $\boldsymbol{W_m} = \mathrm{diag}\{w_{mi}\}$, $i = 1, \ldots, n$ are positive definite matrices of the controller gains.

One important point to note here is that, since the interaction force in the slave side is considered to be zero, hence there is no requirement of including any compensatory term in the master controller for the slave side interaction forces. However, there is an external force applied to the master manipulator. The movement of the master manipulator is commanded by this force, and hence, its inclusion in the slave manipulator controller is necessary for the proper depiction of the transmitted dynamics. Thus, the controller for the slave manipulator has the same structure as the master manipulator controller apart from the extra term for the applied force (delayed signal) in the master arm as follows:

$$\begin{aligned} \boldsymbol{u}_s(t) =& \boldsymbol{M}_s(\boldsymbol{q}_s)\left[-\boldsymbol{K}_s \operatorname{sign}(\boldsymbol{s}_s(t)) - \boldsymbol{W}_s \boldsymbol{s}_s(t) - \boldsymbol{C}_2 \boldsymbol{\sigma}_s(t)\right] \\ &+ \boldsymbol{C}_s(\boldsymbol{q}_s, \dot{\boldsymbol{q}}_s)\dot{\boldsymbol{q}}_s + \boldsymbol{G}_s(\boldsymbol{q}_s) + \boldsymbol{\tau}_h(t-h) \end{aligned} \tag{26}$$

where $\boldsymbol{K}_s = \operatorname{diag}\{k_{si}\}$ and $\boldsymbol{W}_s = \operatorname{diag}\{w_{si}\},\ i = 1, \ldots, n$ are positive definite matrices of the controller gains.

3.3 Closed-Loop System

The closed-loop systems during the reaching phase resulting from the application of the control laws (25) and (26) to (1a) and (1b), respectively, are as follows

$$\begin{aligned} \ddot{\boldsymbol{q}}_m(t) =& -\boldsymbol{K} \operatorname{sign}(\boldsymbol{s}_m(t)) - \boldsymbol{W} \boldsymbol{s}_m(t) - \boldsymbol{C}_2 \boldsymbol{\sigma}_m(t) + \boldsymbol{M}_m^{-1}(\boldsymbol{q}_m)\boldsymbol{\tau}_h(t) \\ &+ \boldsymbol{M}_m^{-1}(\boldsymbol{q}_m)\boldsymbol{d}_m(\boldsymbol{q}_m, \dot{\boldsymbol{q}}_m) \end{aligned} \tag{27a}$$

$$\begin{aligned} \ddot{\boldsymbol{q}}_s(t) =& -\boldsymbol{K} \operatorname{sign}(\boldsymbol{s}_s(t)) - \boldsymbol{W} \boldsymbol{s}_s(t) - \boldsymbol{C}_2 \boldsymbol{\sigma}_s(t) + \boldsymbol{M}_s^{-1}(\boldsymbol{q}_s)\boldsymbol{\tau}_h(t-h) \\ &+ \boldsymbol{M}_s^{-1}(\boldsymbol{q}_s)\boldsymbol{d}_s(\boldsymbol{q}_s, \dot{\boldsymbol{q}}_s) \end{aligned} \tag{27b}$$

Considering the following candidate Lyapunov Function

$$V_s = \frac{1}{2}(\boldsymbol{s}_m^T \boldsymbol{s}_m + \boldsymbol{s}_s^T \boldsymbol{s}_s) \tag{28}$$

$$\begin{aligned} \dot{V}_s =& \boldsymbol{s}_m^T\left[\ddot{\boldsymbol{q}}_m - \ddot{\boldsymbol{q}}_s(t-h) + \boldsymbol{C}_2\boldsymbol{\sigma}_m\right] + \boldsymbol{s}_s^T\left[\ddot{\boldsymbol{q}}_s - \ddot{\boldsymbol{q}}_m(t-h) + \boldsymbol{C}_2\boldsymbol{\sigma}_s\right] \\ =& \boldsymbol{s}_m^T\big[-\boldsymbol{K}_m \operatorname{sign}(\boldsymbol{s}_m) - \boldsymbol{W}_m\boldsymbol{s}_m + \boldsymbol{M}_m^{-1}(\boldsymbol{q}_m)\boldsymbol{\tau}_h(t) - \ddot{\boldsymbol{q}}_s(t-h) \\ &+ \boldsymbol{M}_m^{-1}(\boldsymbol{q}_m)\boldsymbol{d}_m(\boldsymbol{q}_m, \dot{\boldsymbol{q}}_m)\big] + \boldsymbol{s}_s^T\big[-\boldsymbol{K}_s \operatorname{sign}(\boldsymbol{s}_s) - \boldsymbol{W}_s\boldsymbol{s}_s \\ &+ \boldsymbol{M}_s^{-1}(\boldsymbol{q}_s)\boldsymbol{\tau}_h(t-h) - \ddot{\boldsymbol{q}}_m(t-h) + \boldsymbol{M}_s^{-1}(\boldsymbol{q}_s)\boldsymbol{d}_s(\boldsymbol{q}_s, \dot{\boldsymbol{q}}_s)\big] \\ =& -|\boldsymbol{s}_m|^T\boldsymbol{k}_m - \boldsymbol{s}_m^T\boldsymbol{W}_m\boldsymbol{s}_m + \boldsymbol{s}_m^T\boldsymbol{M}_m^{-1}(\boldsymbol{q}_m)\boldsymbol{\tau}_h(t) - \boldsymbol{s}_m^T\ddot{\boldsymbol{q}}_s(t-h) \\ &+ \boldsymbol{s}_m^T\boldsymbol{M}_m^{-1}(\boldsymbol{q}_m)\boldsymbol{d}_m(\boldsymbol{q}_m, \dot{\boldsymbol{q}}_m) - |\boldsymbol{s}_s|^T\boldsymbol{k}_s - \boldsymbol{s}_s^T\boldsymbol{W}_s\boldsymbol{s}_s \\ &+ \boldsymbol{s}_s^T\boldsymbol{M}_s^{-1}(\boldsymbol{q}_s)\boldsymbol{\tau}_h(t-h) + \boldsymbol{s}_s^T\boldsymbol{M}_s^{-1}(\boldsymbol{q}_s)\boldsymbol{d}_s(\boldsymbol{q}_s, \dot{\boldsymbol{q}}_s) \end{aligned} \tag{29}$$

where $\boldsymbol{k} = [k_{m1}\ \ k_{m2} \ldots k_{mn}]^T$ with k_{mi} being the diagonal elements of $\boldsymbol{K}_m$ and $\boldsymbol{k}_s = [k_{s1}\ \ k_{s2} \ldots k_{sn}]^T$ with k_{si} being the diagonal elements of $\boldsymbol{K}_s$ Since $\boldsymbol{M}_m^{-1}(\boldsymbol{q}_m)$, $\boldsymbol{M}_s^{-1}(\boldsymbol{q}_s)$, $\boldsymbol{\tau}_h$, $\ddot{\boldsymbol{q}}_m$ and $\ddot{\boldsymbol{q}}_s$ are bounded as per the assumptions (1)–(3)

the following inequalities can be derived:

$$\boldsymbol{s}_m^T \boldsymbol{M}_m^{-1}(\boldsymbol{q}_m)\boldsymbol{\tau}_h(t) \leq \bar{m}_{1m}|\boldsymbol{s}_m|^T \boldsymbol{\rho} \tag{30a}$$

$$\boldsymbol{s}_m^T \ddot{\boldsymbol{q}}_s(t-h) \leq |\boldsymbol{s}_m|^T \bar{\ddot{\boldsymbol{q}}}_s \tag{30b}$$

$$\boldsymbol{s}_m^T \boldsymbol{M}_m^{-1}(\boldsymbol{q}_m)\boldsymbol{d}_m(\boldsymbol{q}_m, \dot{\boldsymbol{q}}_m) \leq m_{1m}|\boldsymbol{s}_m|^T \bar{\boldsymbol{d}}_m \tag{30c}$$

$$\boldsymbol{s}_s^T \boldsymbol{M}_s^{-1}(\boldsymbol{q}_s)\boldsymbol{\tau}_h(t-h) \leq \bar{m}_{1s}|\boldsymbol{s}_s|^T \boldsymbol{\rho} \tag{30d}$$

$$\boldsymbol{s}_s^T \ddot{\boldsymbol{q}}_m(t-h) \leq |\boldsymbol{s}_s|^T \bar{\ddot{\boldsymbol{q}}}_m \tag{30e}$$

$$\boldsymbol{s}_s^T \boldsymbol{M}_s^{-1}(\boldsymbol{q}_s)\boldsymbol{d}_s(\boldsymbol{q}_s, \dot{\boldsymbol{q}}_s) \leq m_{1s}|\boldsymbol{s}_s|^T \bar{\boldsymbol{d}}_s \tag{30f}$$

Using (30) in (29), the following is derived

$$\begin{aligned} \dot{V}_s \leq & -|\boldsymbol{s}_m|^T \boldsymbol{k}_m - \boldsymbol{s}_m^T \boldsymbol{W}_m \boldsymbol{s}_m + \bar{m}_{1m}|\boldsymbol{s}_m|^T \boldsymbol{\rho} + |\boldsymbol{s}_m|^T \bar{\ddot{\boldsymbol{q}}}_s + m_{1m}|\boldsymbol{s}_m|^T \bar{\boldsymbol{d}}_m \\ & -|\boldsymbol{s}_s|^T \boldsymbol{k}_s - \boldsymbol{s}_s^T \boldsymbol{W}_s \boldsymbol{s}_s + \bar{m}_{1s}|\boldsymbol{s}_s|^T \boldsymbol{\rho} + |\boldsymbol{s}_s|^T \bar{\ddot{\boldsymbol{q}}}_m + m_{1s}|\boldsymbol{s}_s|^T \bar{\boldsymbol{d}}_s \\ \leq & -|\boldsymbol{s}_m|^T (\boldsymbol{k}_m - m_{1m}\boldsymbol{\rho} - \bar{\ddot{\boldsymbol{q}}}_s - m_{1m}\bar{\boldsymbol{d}}_m) - \boldsymbol{s}_m^T \boldsymbol{W}_m \boldsymbol{s}_m \\ & -|\boldsymbol{s}_s|^T (\boldsymbol{k}_s - m_{1s}\boldsymbol{\rho} - \bar{\ddot{\boldsymbol{q}}}_m - m_{1s}\bar{\boldsymbol{d}}_s) - \boldsymbol{s}_s^T \boldsymbol{W}_s \boldsymbol{s}_s \end{aligned} \tag{31}$$

Thus from (31), if the switching gains for the controller are large enough to satisfy

$$\boldsymbol{k}_m > m_{1m}\boldsymbol{\rho} + \bar{\ddot{\boldsymbol{q}}}_s + m_{1m}\bar{\boldsymbol{d}}_m \tag{32a}$$

$$\boldsymbol{k}_s > m_{1s}\boldsymbol{\rho} + \bar{\ddot{\boldsymbol{q}}}_m + m_{1s}\bar{\boldsymbol{d}}_s \tag{32b}$$

then, the time derivative of CLF V_s will satisfy the following

$$\dot{V}_s \leq -\boldsymbol{s}_m^T \boldsymbol{W}_m \boldsymbol{s}_m - \boldsymbol{s}_s^T \boldsymbol{W}_s \boldsymbol{s}_s \leq 0 \tag{32c}$$

which indicates that the sliding surface can be reached in finite time, and the state trajectories can be maintained there for the subsequent times. From (32), the robustness of the controller will increase with higher values of the switching controller gains $\boldsymbol{K}_i,\ i = m, s$, but this high value produces a significant amount of chattering in the control law. This is a compromise at which the robustness of the SMC is achieved.

3.4 Gain Adaptation

The robustness of the sliding mode controller lies in its gain value $\boldsymbol{K}_i$. However, this robustness is achieved at the expense of high chattering and thus higher energy utilization at the input. Although chattering reduction can be achieved by replacing the signum function of the sliding mode controller with a smoother approximation, it often causes deterioration in the controller performance. One very effective method of maintaining controller robustness while reducing chattering is the use of an adaptively tuned gain for the SMC which automatically reduces the controller gain once the states approach steady-state thus eliminating unnecessary use of input energy. The adaptive tuning of the gain with a leakage term [2] is defined as follows

$$\dot{\hat{\boldsymbol{k}}}(t) = \boldsymbol{\Gamma}(|\boldsymbol{s}_i(\boldsymbol{t})| - \boldsymbol{\epsilon}\hat{\boldsymbol{k}}(\boldsymbol{t})) \tag{33}$$

$$\hat{\boldsymbol{k}}(t) = \int_{\boldsymbol{0}}^{\boldsymbol{t}} \dot{\hat{\boldsymbol{k}}}(\boldsymbol{s})\boldsymbol{d}(\boldsymbol{s}) \tag{34}$$

where $i = m, s$ and $\hat{\boldsymbol{k}}(t) = [\hat{k}_j(t)],\ j = 1, \ldots, n$ and $\boldsymbol{K}$ in the control law is replaced with $\hat{\boldsymbol{K}}(t) = \text{diag}\{\hat{k}_j(t)\},\ \ j = 1, \ldots, n$. $\boldsymbol{\Gamma} = \text{diag}\{\gamma_j\}, \gamma_j > 0,\ \ j = 1, \ldots, n$ and $\boldsymbol{\epsilon} = \text{diag}\{\epsilon_j\}, \epsilon_j > 0,\ \ j = 1, \ldots, n$ are user defined parameters.

3.5 Analysis

A new CLF is now defined as follows in order to analyze the system with the adaptively tuned gain:

$$\begin{aligned} V =& V_s + \frac{1}{2}\sum_{\boldsymbol{i=m,s}} \tilde{\boldsymbol{k}}_{\boldsymbol{i}}^{\boldsymbol{T}} \boldsymbol{\Gamma}^{-\boldsymbol{1}} \tilde{\boldsymbol{k}}_{\boldsymbol{i}} \\ =& \frac{1}{2}\sum_{\boldsymbol{i=m,s}} \boldsymbol{s}_{\boldsymbol{i}}^{\boldsymbol{T}} \boldsymbol{s}_{\boldsymbol{i}} + \frac{1}{2}\sum_{\boldsymbol{i=m,s}} \tilde{\boldsymbol{k}}_{\boldsymbol{i}}^{\boldsymbol{T}} \boldsymbol{\Gamma}^{-\boldsymbol{1}} \tilde{\boldsymbol{k}}_{\boldsymbol{i}} \end{aligned} \tag{35}$$

where $\tilde{\boldsymbol{k}}_{\boldsymbol{i}} = \hat{\boldsymbol{k}}_{\boldsymbol{i}} - \boldsymbol{k}_{\boldsymbol{i}},\ i = m, s$ and $0 < \boldsymbol{k}_{\boldsymbol{i}} < \infty,\ \boldsymbol{k}_{\boldsymbol{i}} \in \mathbb{R}^n,\ i = m, s$ is the arbitrary value to which the adaptively tune gain converges to.

The following Lemma will be used in the further analysis

Lemma 1 *For real vectors* $\tilde{\boldsymbol{k}}_i, \hat{\boldsymbol{k}}_, k_i > 0, i = m, s$ *and positive definite diagonal matrix* $\boldsymbol{\epsilon} \in \mathbb{R}^{n\times n}$*, if* $\tilde{\boldsymbol{k}}_i = \hat{\boldsymbol{k}}_i - k_i$ *then* $\tilde{\boldsymbol{k}}_i^T \boldsymbol{\epsilon}\hat{\boldsymbol{k}}_i \geq \frac{1}{2}\tilde{\boldsymbol{k}}_i^T \boldsymbol{\epsilon}\tilde{\boldsymbol{k}}_i - k_i^T \boldsymbol{\epsilon} k_i$

Proof The proof can be found in [1], page 111.

Taking time derivative of V, and using (32c), (33), and Lemma (1) , the following can be derived

$$
\begin{aligned}
\dot{V} \leq & -\sum_{i=m,s} \boldsymbol{s}_i^T \boldsymbol{W}_i \boldsymbol{s}_i + \sum_{i=m,s} \left(\tilde{\boldsymbol{k}}_i^T \boldsymbol{\Gamma}^{-1} \dot{\tilde{\boldsymbol{k}}}_i\right) \\
\leq & -\sum_{i=m,s} \boldsymbol{s}_i^T \boldsymbol{W}_i \boldsymbol{s}_i + \sum_{i=m,s} \left(\tilde{\boldsymbol{k}}_i^T \boldsymbol{\Gamma}^{-1} \boldsymbol{\Gamma}(|\boldsymbol{s}_i| - \boldsymbol{\epsilon} \hat{\boldsymbol{k}}_i)\right) \\
\leq & -\sum_{i=m,s} \boldsymbol{s}_i^T \boldsymbol{W}_i \boldsymbol{s}_i + \sum_{i=m,s} \left(\tilde{\boldsymbol{k}}_i^T |\boldsymbol{s}_i| - \tilde{\boldsymbol{k}}_i^T \boldsymbol{\epsilon} \hat{\boldsymbol{k}}_i)\right) \\
\leq & -\sum_{i=m,s} \boldsymbol{s}_i^T \boldsymbol{W}_i \boldsymbol{s}_i + \frac{1}{2} \sum_{i=m,s} \left(\tilde{\boldsymbol{k}}_i^T \boldsymbol{\epsilon} \tilde{\boldsymbol{k}}_i - \boldsymbol{k}_i^T \boldsymbol{\epsilon} \boldsymbol{k}_i\right) \\
\leq & -\sum_{i=m,s} \boldsymbol{s}_i^T \boldsymbol{W}_i \boldsymbol{s}_i - \frac{1}{2} \sum_{i=m,s} \boldsymbol{k}_i^T \boldsymbol{\epsilon} \boldsymbol{k}_i + \frac{1}{2} \sum_{i=m,s} \tilde{\boldsymbol{k}}_i^T \boldsymbol{\epsilon} \tilde{\boldsymbol{k}}_i \\
\leq & -\sum_{i=m,s} \lambda_{\min}(\boldsymbol{W}_i) \boldsymbol{s}_i^T \boldsymbol{s}_i - \sum_{i=m,s} \lambda_{\min}(\boldsymbol{\Gamma} \boldsymbol{\epsilon}) \boldsymbol{k}_i^T \boldsymbol{\Gamma}^{-1} \boldsymbol{k}_i + \frac{1}{2} \sum_{i=m,s} |\tilde{\boldsymbol{k}}_i^T \boldsymbol{\epsilon} \tilde{\boldsymbol{k}}_i| \\
\leq & -\eta \left(\sum_{i=m,s} \boldsymbol{s}_i^T \boldsymbol{s}_i + \sum_{i=m,s} \boldsymbol{k}_i^T \boldsymbol{\Gamma}^{-1} \boldsymbol{k}_i \right) + \frac{1}{2} \xi_k \\
\leq & -2\eta V + \frac{1}{2} \xi_k
\end{aligned} \tag{36}
$$

where $\lambda_{\min}(\boldsymbol{A})$ indicates the minimum eigenvalue of matrix $\boldsymbol{A}$, $\eta = \min(\lambda_{\min}(\boldsymbol{W}_i),\ \lambda_{\min}(\boldsymbol{\Gamma}\boldsymbol{\epsilon})),\ i = m, s$ and $\frac{1}{2}\xi_k = \frac{1}{2}\sum_{i=m,s} \tilde{\boldsymbol{k}}_i^T \boldsymbol{\epsilon} \tilde{\boldsymbol{k}}_i,\ i = m, s$. Thus for $V(0) > \frac{\xi_k}{4\eta}$ and $\frac{\xi_k}{4\eta} < 1$, $V(t)$ will be a decreasing function, indicating the stability of the system.

4 Simulation Results

The proposed controllers (25), (26) are tested via simulation for the bilateral master-slave operation of two 2DoF manipulators having identical structures as given in (2).

A Cartesian force, as shown in Fig. 2, is applied to the end-effector of the master manipulator. The resultant joint motions are transmitted to the slave manipulator where the aim is to synchronize with the motion of the master manipulator. The parameters of the manipulators are as follows: $m_{1i} = m_{2i} = 1$ kg, $l_{1i} = l_{2i} = 1$ m, $g = 9.81$ kg m/s^2.

The controller gains used in the simulation are $C_1 = 2,\ C_2 = 0.001$. The parameters for the adaptive law for the gain are $\Gamma = 100$, $\epsilon = 0.1$, $W = 2$.

The controller can withstand a communication delay up to 2.5 s, beyond which its performance deteriorates with the given control parameters. Parametric uncertainty in the form of a 0.01 kg deviation of the nominal mass of the manipulator joints

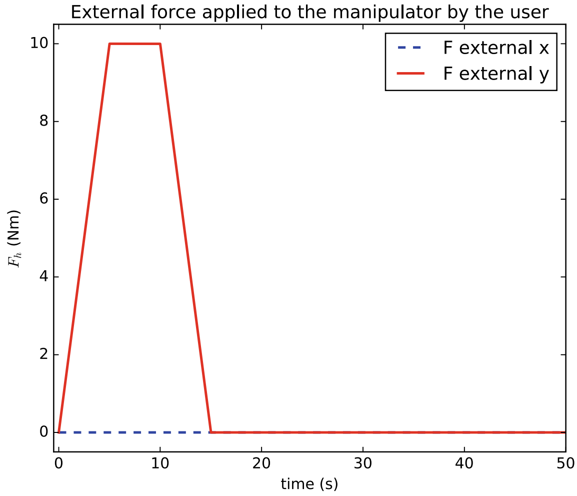

Fig. 2 External force applied by the user

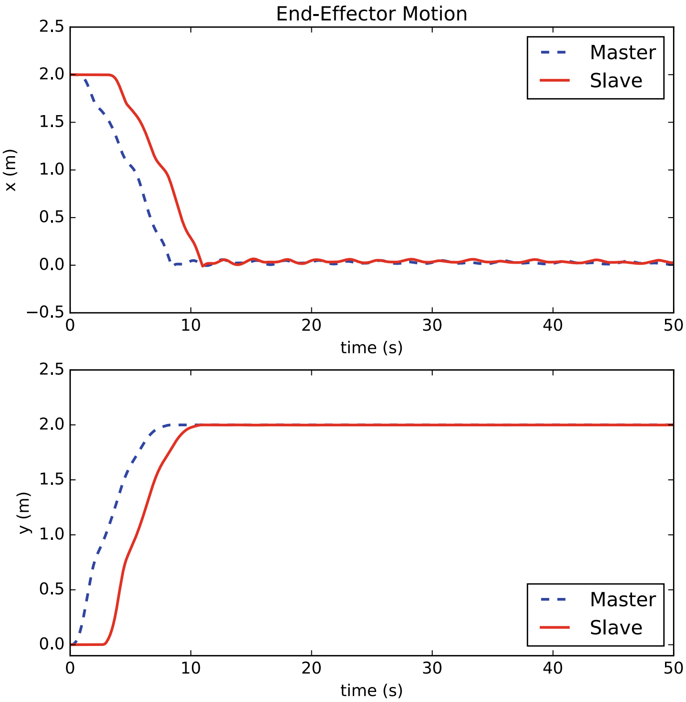

Fig. 3 End-effector trajectory

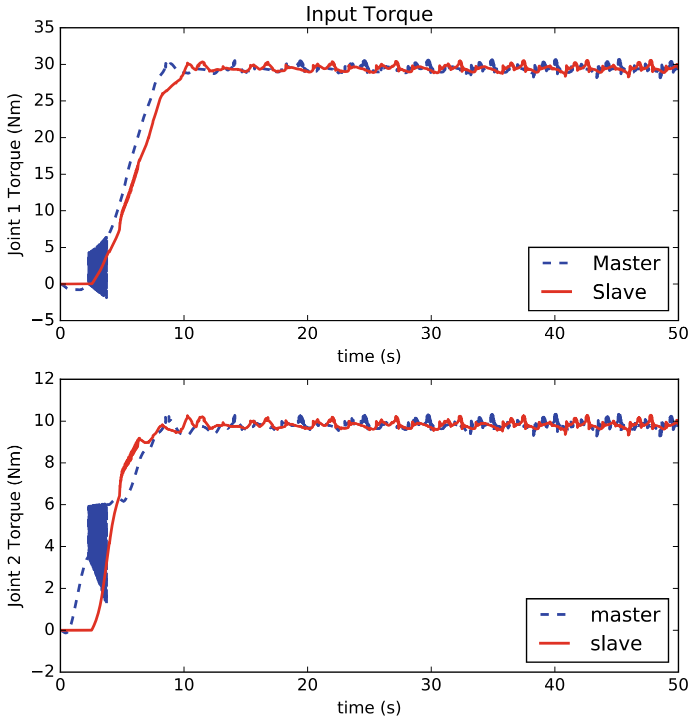

Fig. 4 Input torques

from the actual mass is considered. Moreover, a uniform random noise having limits ± 0.0001rad is added to the measurements of positions.

From Fig. 3, it can be observed that despite the 2.5 s delay, the slave manipulator is following the trajectory of the master manipulator with sufficient accuracy which is also reflected in Fig. 6 which shows the joint angular position error between the master and the slave. From Fig. 4, it is clear that the input torques for all the joints in both master and slave manipulator do not suffer from any high magnitude, high-frequency chattering, unlike the conventional sliding mode controllers. This can be attributed to the adaptively tuned gain as shown in Fig. 8, which is initially high when the system error is high, and as the tracking error converges to zero, the gain also converges to a small value (Figs. 5 and 7).

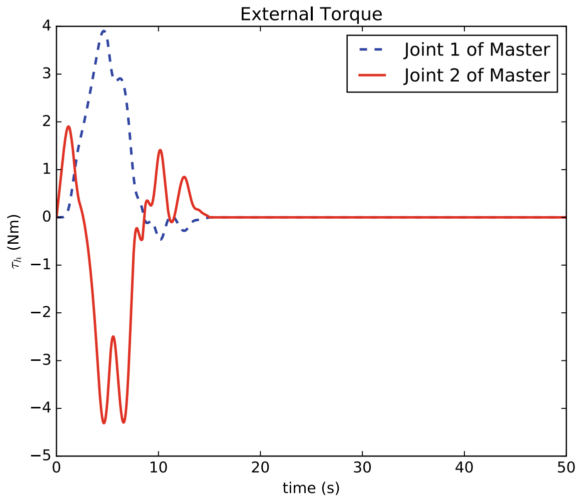

Fig. 5 External torques on master manipulator

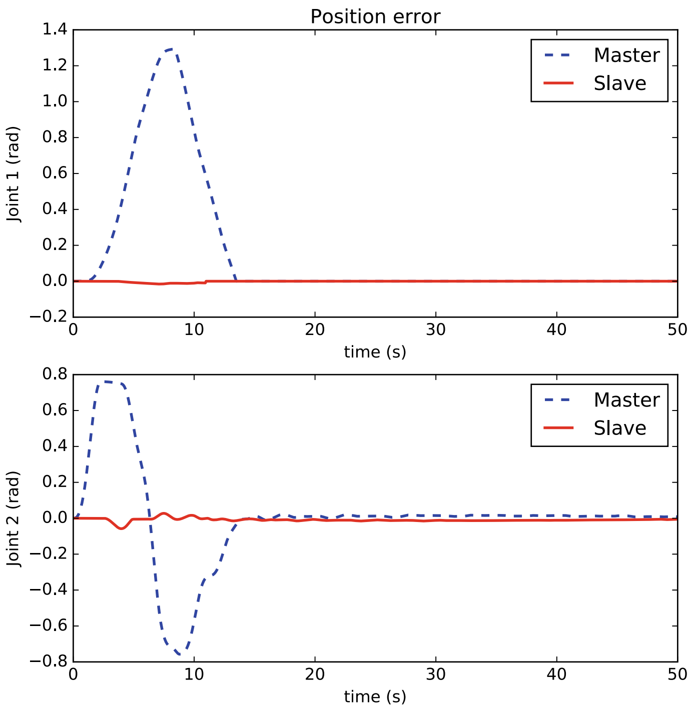

Fig. 6 Tracking error

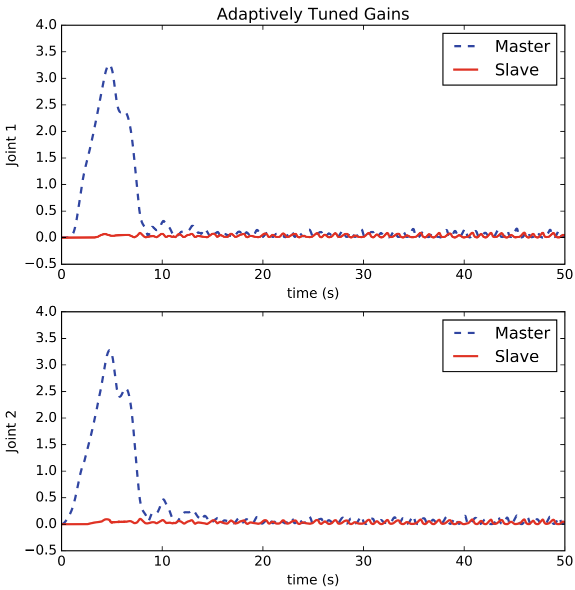

Fig. 7 Adaptively tuned gain K

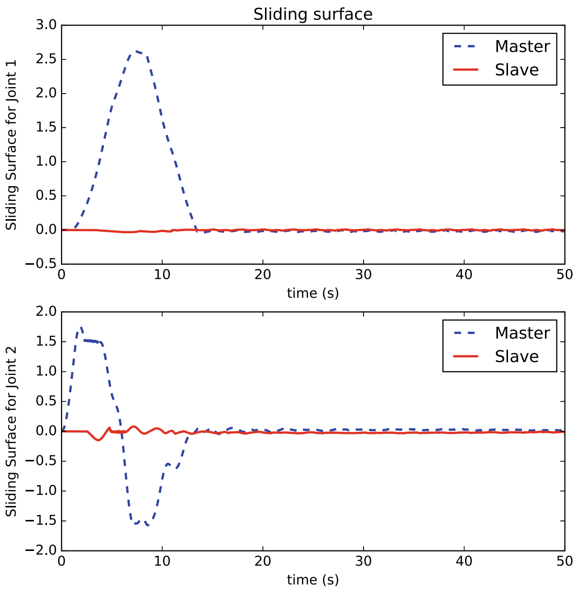

Fig. 8 Sliding surface

5 Conclusion

The proposed adaptive sliding mode controller for bilateral telemanipulation with a delay has a simple structure that is easy to implement. In presence of uncertainty and a delay of up to 2.5 s, the controller shows good performance without any requirements of re-tuning its parameters. The primary analysis regarding the stability of the controller shows that it is robust and can be used even when uncertainty bounds (parametric and external disturbances) are unknown. This can be attributed to the adaptive tuning of the switching gain of the controller, which increases with increasing tracking error and vice versa. Thus, under steady-state conditions, the gain remains at a very low value which prevents the unnecessary use of input energy and also prevents high amplitude and high-frequency chattering. Future work for the proposed method is to perform further analysis to gain detailed information regarding the delay tolerance of the system, and the same research can be extended to multilateral telemanipulation.

Acknowledgements This work has been supported by Scheme for Promotion of Academic and Research Collaboration (SPARC), MHRD, Government of India, no. SPARC/2018–2019/P1087/SL.

References

1. Adhikary, N.: Design of a few backstepping sliding mode based robust control techniques for robot manipulators. Ph.D. thesis (2017)
2. Blažič, S., Matko, D., Škrjanc, I.: A new leakage term in the adaptive law. IFAC Proc. Vol. **41**(2), 8913–8918 (2008). https://doi.org/10.3182/20080706-5-KR-1001.01506 (17th IFAC World Congress)
3. Cruz-Ortiz, D., Chairez, I., Poznyak, A.: Robust control of a master-slave manipulator under restricted task-space. In: Hernandez, E.E., Keshtkar, S., Valdez, S.I. (eds.) Industrial and Robotic Systems, pp. 240–248. Springer International Publishing, Cham (2020)
4. Huang, F., Zhang, W., Chen, Z., Tang, J., Song, W., Zhu, S.: Rbfnn-based adaptive sliding mode control design for nonlinear bilateral teleoperation system under time-varying delays. IEEE Access **7**, 11905–11912 (2019)
5. Moreau, R., Pham, M., Tavakoli, M., Le, M., Redarce, T.: Sliding-mode bilateral teleoperation control design for master-slave pneumatic servo systems. Control Eng. Pract. **20**(6), 584–597 (2012). https://doi.org/10.1016/j.conengprac.2012.02.003, http://www.sciencedirect.com/science/article/pii/S0967066112000275
6. Murray, R.M., Li, Z., Sastry, S.S., Sastry, S.S.: A Mathematical Introduction to Robotic Manipulation. CRC Press, Boca Raton (1994)
7. Wang, Z., Chen, Z., Liang, B., Zhang, B.: A novel adaptive finite time controller for bilateral teleoperation system. Acta Astronautica **144**, 263–270 (2018). https://doi.org/10.1016/j.actaastro.2017.12.046, http://www.sciencedirect.com/science/article/pii/S0094576517301224
8. Wang, Z., Chen, Z., Zhang, Y., Yu, X., Wang, X., Liang, B.: Adaptive finite-time control for bilateral teleoperation systems with jittering time delays. Int. J. Robust Nonlinear Control **29**(4), 1007–1030 (2019)
9. Yang, H., Liu, L., Wang, Y.: Observer-based sliding mode control for bilateral teleoperation with time-varying delays. Control Eng. Pract. **91** (2019). https://doi.org/10.1016/j.conengprac.2019.07.015, http://www.sciencedirect.com/science/article/pii/S0967066119301145

10. Yang, L., Chen, Y., Liu, Z., Chen, K., Zhang, Z.: Adaptive fuzzy control for teleoperation system with uncertain kinematics and dynamics. Int. J. Control Autom. Syst. **17**(5), 1158–1166 (2019)
11. Yang, X., Hua, C., Yan, J., Guan, X.: A new master-slave torque design for teleoperation system by t-s fuzzy approach. IEEE Trans. Control Syst. Technol. **23**(4), 1611–1619 (2015)
12. Zhai, D., Xia, Y.: Adaptive control for teleoperation system with varying time delays and input saturation constraints. IEEE Trans. Industr. Electron. **63**(11), 6921–6929 (2016)
13. Zhang, J., Liu, W., Gao, L., Li, L., Li, Z.: The master adaptive impedance control and slave adaptive neural network control in underwater manipulator uncertainty teleoperation. Ocean Eng. **165**, 465–479 (2018). https://doi.org/10.1016/j.oceaneng.2018.07.055, http://www.sciencedirect.com/science/article/pii/S0029801818313763
14. Zhao, L., Zhang, H., Yang, Y., Yang, H.: Integral sliding mode control of a bilateral teleoperation system based on extended state observers. Int. J. Control Autom. Syst. **15**(5), 2118–2125 (2017)